ACADEMIA ROMÂNĂ
*Revue Roumaine de Chimie*
https://www.icf.ro/rrch/

*Rev. Roum. Chim.*,
**2026**, *71*(5–6), 333–342
DOI: 10.33224/rrch.2026.71.5-6.04

*Dedicated to Professor Alexandru T. Balaban*
*on the occasion of his 95th anniversary*

# MECHANICAL AND CHEMICAL PROPERTIES OF ROSIN-BASED HYBRID RESINS**

Ion NEDA,*[a] Martin Heiko FRANZ,[a] Ion CIUCA,[b] Walter Robert LINKE,[c] Michael Ryan HANSEN,[c] Dumitru BOLCU[d] and Marius Marinel STANESCU[d]

[a] Institut für Anorganische und Analytische Chemie, Technische Universität Braunschweig, Hagenring 30, D-38106 Braunschweig, Germany
[b] Faculty of Material Science and Engineering, University Politehnica of Bucharest, 313 Splaiul Independentei, 060042, Sector 6, Bucharest, Roumania
[c] Institut für Physikalische Chemie, Universität Münster, Correnstraße 28/30, 48149 Münster, Germany
[d] Faculty of Mechanics, University of Craiova, 107 Calea Bucuresti, 200512, Craiova, Roumania

*Received December 18, 2025*

The pursuit for sustainable alternatives to petroleum-based polymer materials has become hugely important. Derived from coniferous trees, rosin stands out as an excellent choice that combine economic aspects and outstanding environmental compatibility. A novel hybrid resin was developed, integrating Resoltech 1050 epoxy resin and its complementary Resoltech 1055 hardener with natural rosin resin. This research explored the mechanical properties and chemical bonding characteristics of hybrid resins. Increasing the rosin content resulted in a reduction in stiffness and strength properties. Modulus of elasticity, tensile strength, and elongation at break were evaluated. Complementing these findings, chemical analyses using solid-state 13C NMR and IR spectroscopy demonstrated that the hybrid resins undergo an initial ionic bonding stage between the rosin and epoxy resin, followed by the formation of covalent bonds during curing. Maintaining performance and versatility, the innovative hybrid resins represent a step forward in advancing renewable material technologies.

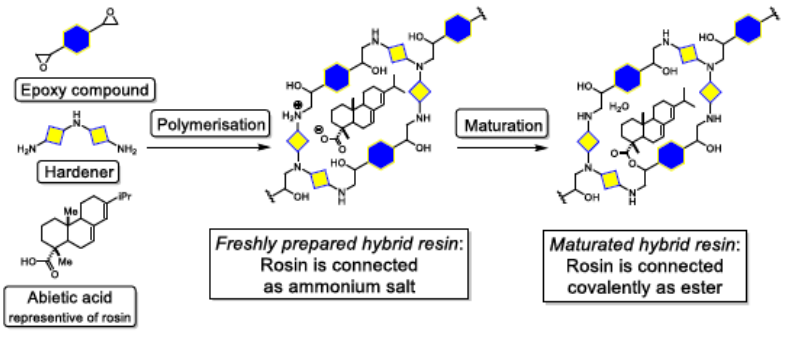


## INTRODUCTION

Rosin is a natural resin that is extracted from pine trees and can be used to produce hybrid resins, which in turn are starting materials for the production of composite materials. It has the advantage of being renewable and has a very low price, more than 10 times lower than synthetic

* Corresponding author: i.neda@tu-braunschweig.de
** Supplementary information on https://www.icf.ro/rrch ; https://revroum.lew.ro

resins. Since the major component is abietic acid, which gives the hybrid resin good hydrophobic properties,[1] rosin can be used to preserve wood, as well as to increase the water resistance of wood joints.[2] Thus, the treatment of poplar wood with solutions obtained by dissolving rosin in different concentrations in ethanol has been proposed. Using a 20% rosin solution resulted in a 20% increase in modulus of elasticity and a 30% increase in compressive strength.[3] Due to its unique properties such as hydrophobicity, biocompatibility and chemical reactivity, rosin is used in a wide range of products such as emulsifier,[4] waterproofing agent and insulating material.[5] It is also used for soap making, printing inks, surface coatings, adhesives and rubber additives, but also for polymer synthesis as a natural filler or source of monomers.[6]

An up-to-date status on rosin presenting its intrinsic characteristics, processing and development of material production for ecological science has recently been reported.[7] The use of rosin to improve the mechanical properties of epoxy resins has been demonstrated.[8] The influence of resin mixing methods on properties such as density, hardness or tensile-compressive behavior was studied. A comparative study was carried out between composites based on rosin imide-diacid reinforced epoxy resin and trimellitic anhydride imide-diacid based composites.[9] A rosin anhydride reinforced epoxy resin composite laminate and reinforced with carbon fiber was also studied.[10] Performance comparable to that of the gasoline-based commercial equivalent was achieved in terms of mechanical properties related to interlaminar rupture and compressive strength after impact.

As shown, rosin is a widely used natural resin that is attractive due to its availability, price and biodegradability. This motivated the idea of combining it with a synthetic epoxy resin / hardener (Resoltech 1050 epoxy resin and Resoltech 1055 hardener). To understand how the components of the insoluble hybrid resins are chemically linked, they were analyzed using solid-state NMR and IR spectroscopy. These two methods are chosen since the resins is insoluble in all solvents.

## RESULTS AND DISCUSSION

### Mechanical properties

Figures 1a–c shows the characteristic curves for representative samples of the three types of hybrid resins. The ultimate tensile strength (UTS), Young's modulus (E) and percentage elongation at fracture ($A_f$) were determined. The experimental results for the sets of specimens from the three hybrid resins, obtained based on tensile stress, are presented in Table 1. Figures 2a–c shows the force-deformation diagram for a representative sample of the three types of hybrid resins. The maximum force ($F_{max}$), deformation at maximum force ($L_{max}$) and tension at maximum force ($\sigma_{max}$) were determined. Maximum load $F_{max}$ [N] and maximum extension $L_{max}$ [mm] obtained from the compressive stress for the three sets of cubes are shown in Table 2.

Comparison of experimental results shows a significant change in mechanical properties when changing the proportion of epoxy resin and natural resins (Table 1, Fig. 1). Thus, for the resin with 45% rosin, the highest values of the mechanical properties are obtained. Compared to this, for 55% rosin resin the breaking strength is 48% and the elastic modulus is 34%, and for the 65% rosin resin the breaking strength is 15% and the elastic modulus is only 2%. A significant decrease in mechanical properties is observed with increasing percentage of rosin in the hybrid resin. Hybrid resins with a higher proportion of epoxy resin have superior mechanical properties, but there is no proportionality between the tensile strength or modulus of elasticity and the volume proportion of epoxy resin. The characteristic curves giving the dependence of stress and specific strain differ greatly for the three types of hybrid resins. Although all exhibit nonlinearities from the beginning of stress, in the case of the 65% rosin resin a flow phenomenon occurs, the elongation increases greatly at a stress increase of only 1 MPa.

*Table 1*

Modulus of elasticity, tensile strength and elongation at breaking for the three sets of tensile specimens

| Volume ratio of rosin | Modulus of elasticity | Tensile strength | Elongation at breaking |
|---|---|---|---|
| | $E$ [*MPa*] | $R_m$ [*MPa*] | $A$ [%] |
| 45% | 870 ± 41 | 17.2 ± 0.85 | 3.6 ± 0.21 |

| | | | |
|---|---|---|---|
| 55% | 300 ± 19 | 8.3 ± 0.61 | 10.4 ± 0.62 |
| 65% | 20 ± 4 | 2.5 ± 0.38 | 30.1 ± 2.45 |

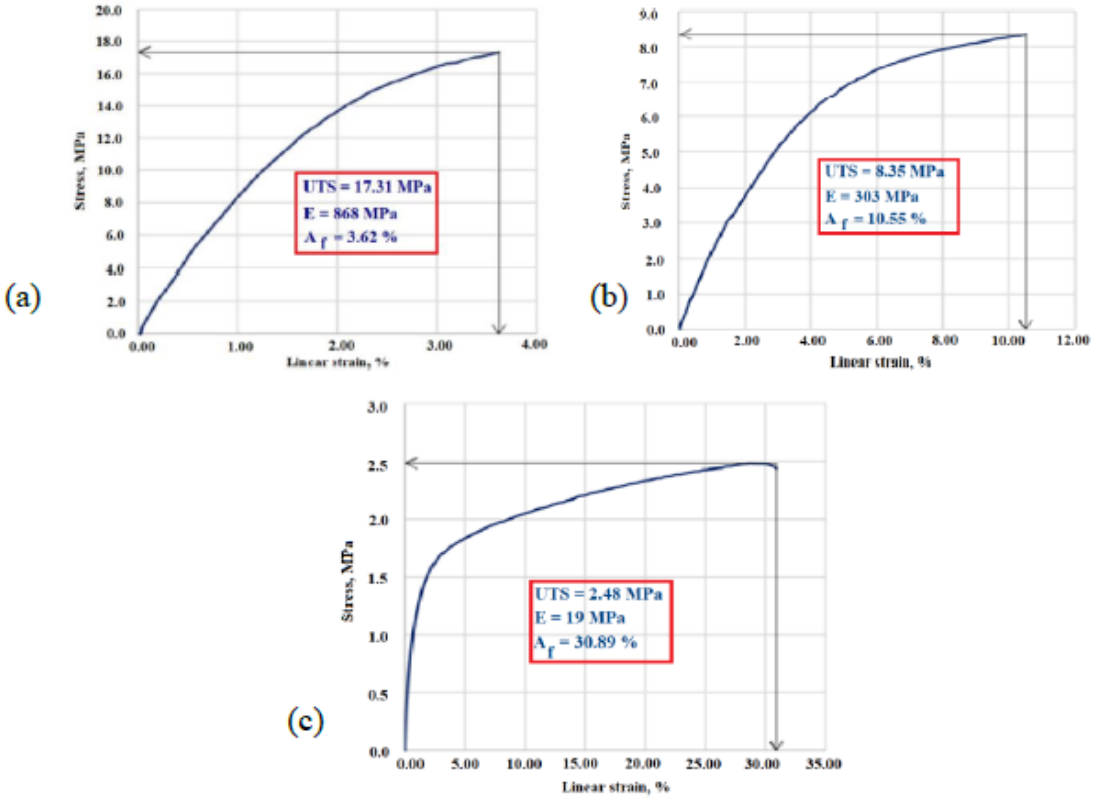


Fig. 1 – Characteristic curve for a representative sample from the combination of: a) 45% rosin and 55% epoxy resin; b) 55% rosin and 45% epoxy resin; c) 65% rosin and 35% epoxy resin. The test speed was 50 mm/min.

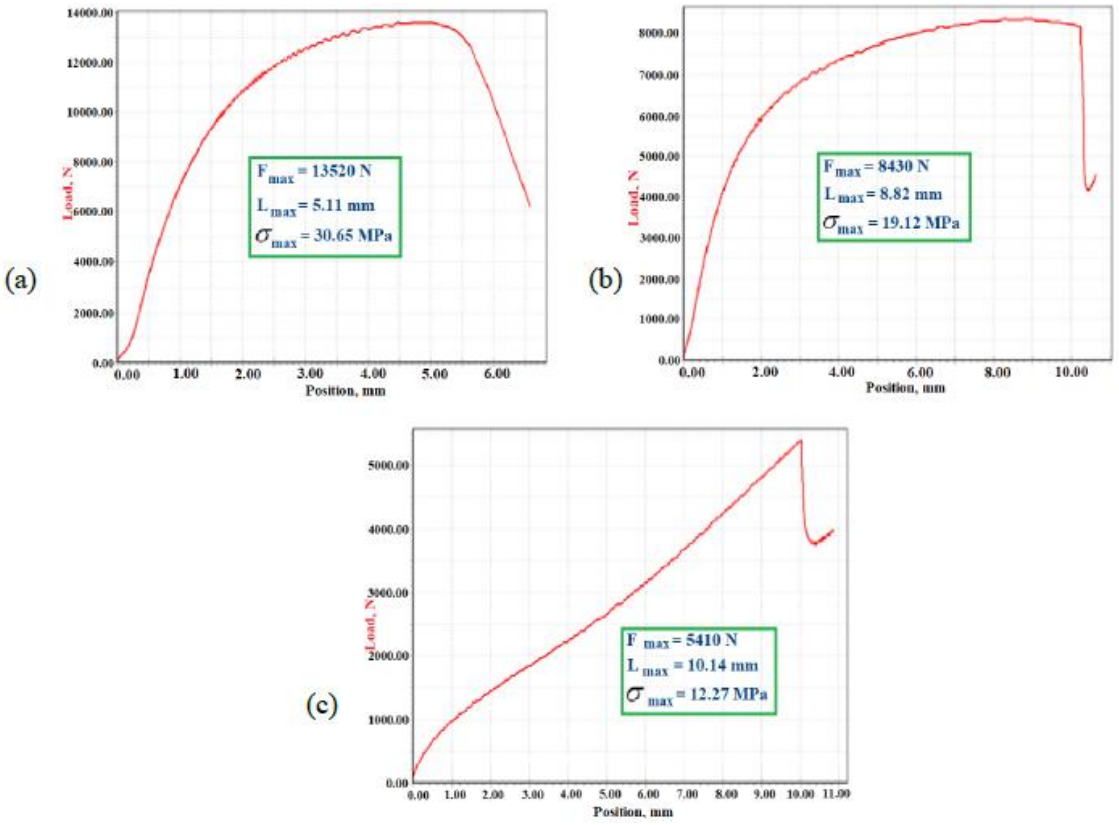

Fig. 2 – Force-deformation diagram for a representative sample of the combination of: a) 45% rosin and 55% epoxy resin; b) 55% rosin and 45% epoxy resin; c) 65% rosin and 35% epoxy resin. The increase of loading force was 250 N/s.

*Table 2*

Maximum load and maximum extension values obtained based on compressive stress for the three sets of cubes

| Volume ratio of rosin | $F_{max}$ maximum load | $L_{max}$ Maximum extension at $F_{max}$ | $\sigma_{max}$ Maximum tensile strength |
|---|---|---|---|
| | [N] | [mm] | [MPa] |
| 45% | 13500 ± 500 | 5.1 ± 0.22 | 30.6 ± 1.15 |
| 55% | 8400 ± 410 | 8.8 ± 0.34 | 19.1 ± 0.93 |
| 65% | 5400 ± 270 | 10.1 ± 0.41 | 12.2 ± 0.62 |

Similar conclusions are obtained in the case of compressive stress, with the hybrid resin with 45% rosin having the best behavior (Table 2, Fig. 2). Compared to this, for the resin with 55% rosin the maximum strength is 62% and for the resin with 65% rosin the maximum strength is 40%. For all the studied resins, the maximum stresses that appeared in compression had higher values than those of the breaking strengths that appeared in tensile stress. Therefore, it is indicated that materials using rosin-based hybrid resins are used for the manufacture of components that are particularly stressed in compression. The use of a volume proportion higher than 65% Rosin in the composition of the hybrid resin produces a sharp decrease in the mechanical properties and a long duration of the polymerization time. These aspects make the resulting hybrid resin uninteresting for use as a matrix in the manufacture of composite materials.

## Structural characterization from liquid and solid-state 13C NMR and IR experiments

Liquid $^{13}C$ NMR experiments for the starting materials (rosin, Resoltech 1050 and Resoltech 1053) and solid-state $^{13}C$ NMR experiments for some hybrid resins were recorded. In addition, $^{1}H$ NMR experiments were also recorded for the starting materials. $^{1}H$ NMR experiment for rosin shows beside signals for aliphatic and vinylic protons (σ = 5.9–5.7 ppm, 5.4–5.2 ppm, 5.0–4.8 ppm the carboxylic proton (σ = 9.95 ppm) as a broad singlet. In case of the epoxy compound signals for the 1,4-substituted aryl units are clearly visible (σ = 7.2–7.05 ppm, 6.9–6.8 ppm). The hardener, Resoltech 1053, has a broad singlet which can be assigned to the (free) amino groups (σ = 1.83 ppm). Furthermore, the hardener has signals at σ = 4.0–2.5 ppm and 1.25–0.75 ppm.

Figure 3 summarizes the liquid- and solid-state $^{13}C$ NMR spectra for all studied samples. The solid-state $^{13}C\{^{1}H\}$ CP/MAS NMR spectrum for the hybrid resins containing 65 % rosin in Fig. 3a includes a new $^{13}C$ signal at $\delta = 177.7$ ppm (highlighted with a black box) that is not present for any of the starting materials. This new $^{13}C$ signal is likely generated by the spatial proximity of the deprotonated carboxyl group of abietic acid to the hydroxyl group of the epoxy resin during the polymerisation process, causing a change to lower ppm values for the chemical shift of these carbon nuclei. The adjacent $^{13}C$ peak at $\delta = 185.4$ ppm is due to the unreacted acid group of abietic acid. The presence of this peak indicates that the reaction is not quantitative. By normalizing the $^{13}C$ signal intensities of the different samples to the signal at $\delta = 157.0$ ppm (from Resoltech 1050, chosen due to its small and consistent linewidth eliminating intensity differences caused by different sample amounts in the MAS rotor), we can show qualitatively that an increase in rosin content results in more abietic acid coordinating with the epoxy resin. Furthermore, the signal intensity of the aliphatic carbons is rising with a higher rosin content because this signal area is dominated by resonances from rosin (Fig. 3a).

In addition to the samples shown in Fig. 3b also aged samples with a rosin content of 50% and 65% were investigated. An important and noticeable difference in Fig. 4a is the presence of a new $^{13}C$ signal at $\delta = 172.3$ ppm in addition to an intensity reduction of the signal at $\delta = 177.7$ ppm. This shows that the ageing of the hybrid resin results in the formation of a new ester bond. The $^{13}C\{^{1}H\}$ RINEPT NMR spectra in Fig. 4b further support this observation as the fresh 65% rosin sample did not show any $^{13}C$ signals in the $^{13}C\{^{1}H\}$ RINEPT

NMR spectra whereas the corresponding aged samples do, *i.e.*, the aged sample includes mobile aliphatic components.[14,15]

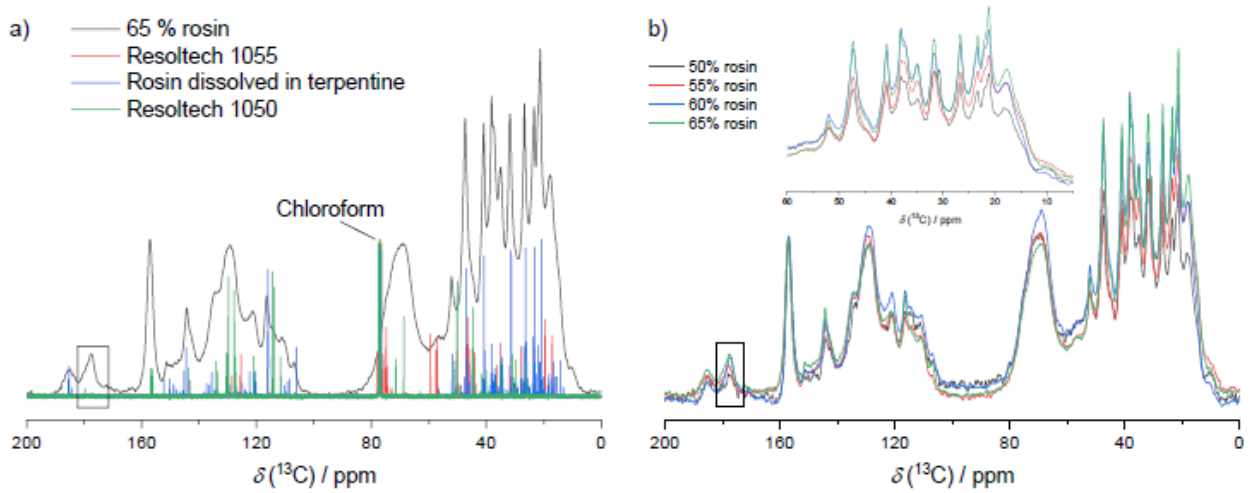


Fig. 3 – a) Solid-state $^{13}C\{^{1}H\}$ CP/MAS NMR spectra of the compound with 65% rosin content (black) compared to the liquid-state $^{13}C$ NMR spectra of the rosin and terpentine mixture (blue), Resoltech 1055 (red), and Resoltech 1050 (green); b) Comparison of solid-state $^{13}C\{^{1}H\}$ CP/MAS NMR spectra for the 50–65% rosin samples normalized to the $^{13}C$ signal at 157.0 ppm. The inset shows the region from 0 to 60 ppm. All spectra were acquired using a magnetic field strength of 7.05 T and a MAS frequency of 10.0 kHz.

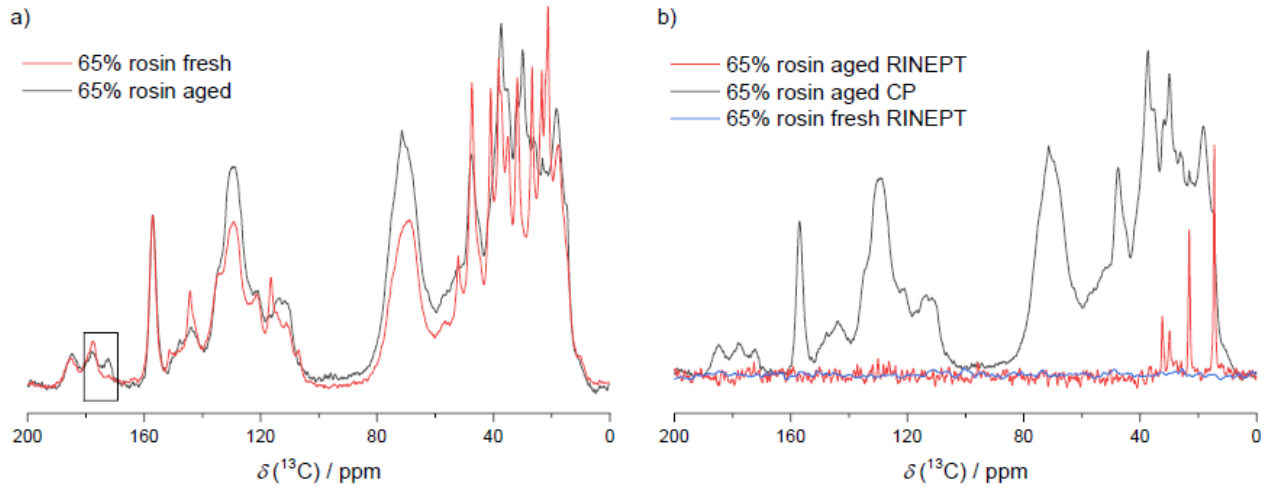


Fig. 4 – a) Comparison of the solid-state $^{13}C\{^{1}H\}$ CP/MAS NMR spectra of the aged and fresh sample with a rosin content of 65%; b) Fresh and aged $^{13}C\{^{1}H\}$ RINEPT and CP/MAS NMR spectra of the samples with a rosin content of 65 % overlayed. All spectra were acquired using a magnetic field strength of 7.05 T and a MAS frequency of 10.0 kHz.

## Infrared spectroscopy

The chemical structure of the produced hybrid resins based on rosin and synthetic epoxy resins were further investigated using infrared spectroscopy (IR). Rosin is a mixture of structurally similar di-terpenes, most of which have a tricyclic basic structure. In addition to the tricyclic structure, characteristic structural elements are a carboxyl group and some double bonds, usually two, which are in conjugation. In addition, there are some aliphatic side chains.[16] The main component of colophony is the abietic acid. Other components of the same mass and similar structure are levopimaric acid, palustric acid and neoabietic acid, which differ in the position of the double bonds. Consequently, the IR spectrum of rosin is dominated by the carboxyl group (Fig. 5), which is located at 1689 $cm^{-1}$. Above this there are strong bands at 2925 $cm^{-1}$ and 2866 $cm^{-1}$, which emphasize the aliphatic structure, and a strong band at 1273 $cm^{-1}$. A detailed description of the IR spectrum of the epoxy resin

based on Resoltech 1050 can be found in the literature.[11]

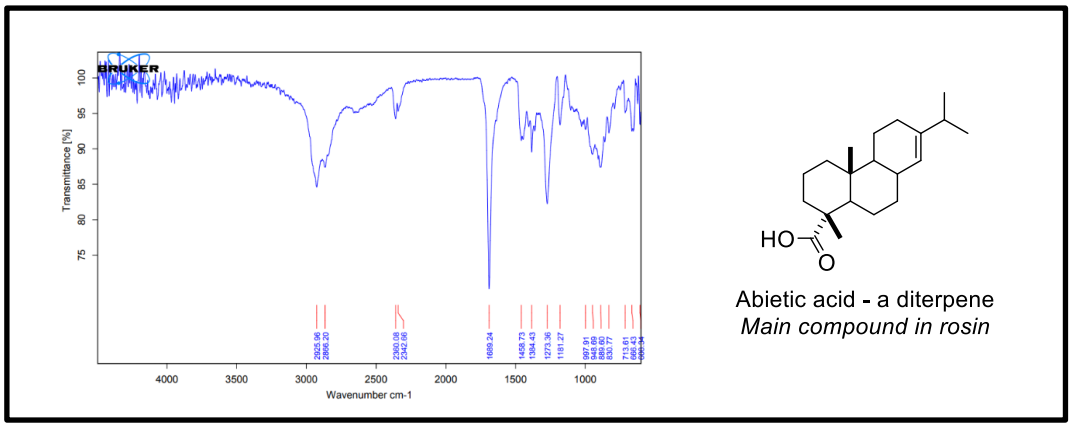


Fig. 5 – IR spectrum of rosin used for the preparation of the composite materials and the structure of abietic acid as the main compound of rosin.

As expected, the IR spectra of the composite materials produced are similar at first glance. The bands at 1175 $cm^{-1}$, 1100 $cm^{-1}$ and 1038 $cm^{-1}$ become smaller as the proportion of rosin increases. In contrast, the signals at 1240 $cm^{-1}$, 1380 $cm^{-1}$, 1450 $cm^{-1}$, 1510 $cm^{-1}$ and 1720 $cm^{-1}$ become more dominant. The signal pair at 2920 $cm^{-1}$ and 2860 $cm^{-1}$ follows this trend (Fig. 6). The observation suggests that the first group represents the epoxy resin, whereas the second group is associated with the embedded rosin. It should be noted that the dominant band of free rosin is no longer observed at 1689 $cm^{-1}$.

The first group of bands can be explained by the product of epoxy resin and hardener, which contains ether groups and hydroxyalkyl groups. The bands are in the expected range. The acids of the rosin seem to be present as carboxylates and form ammonium salts with the amino groups of the resin. The band at 1720 $cm^{-1}$ could be an indication that ester bonds are formed between the hydroxyl groups of the resin and the acids of the rosin.[17] This would be a covalent bond between the rosin and the synthetic epoxy resin.

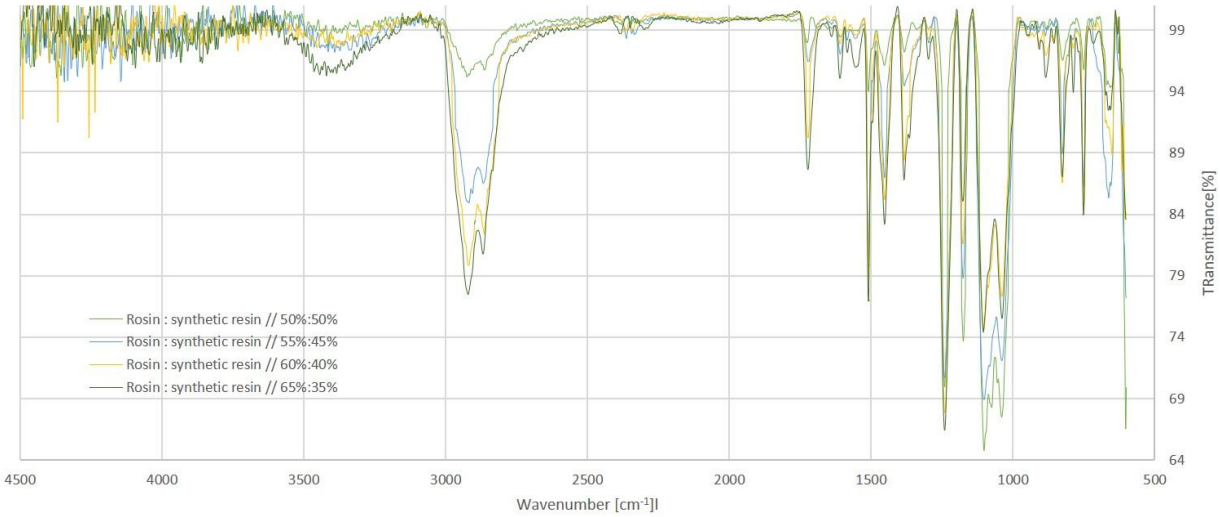


Fig. 6 – IR spectra of composite with different ratio: a) 50% rosin an 50% epoxy resin; b) 55% rosin an 45% epoxy resin; c) 60% rosin an 40% epoxy resin; d) 65% rosin an 35% epoxy resin.

The ageing behavior of the composite materials was investigated using infrared (IR) spectroscopy on two examples (Figs. 7 and 8). Two mixture ratios of colophony to epoxy resin of 1:1 and 2:1 were measured. Essentially, the bands already known from the fresh hybrid resin are visible. In addition, a new band at a wavenumber of 1742 $cm^{-1}$ can be observed in both cases. The band at 1454 $cm^{-1}$ is

also relatively more intense. In addition, the very broad band at 3380 $cm^{-1}$ is much more pronounced compared to the fresh sample. The band at 1742 $cm^{-1}$ is a strong spectroscopic indication that the acids of the rosin are covalently bound to the synthetic epoxy resin during the ageing process.

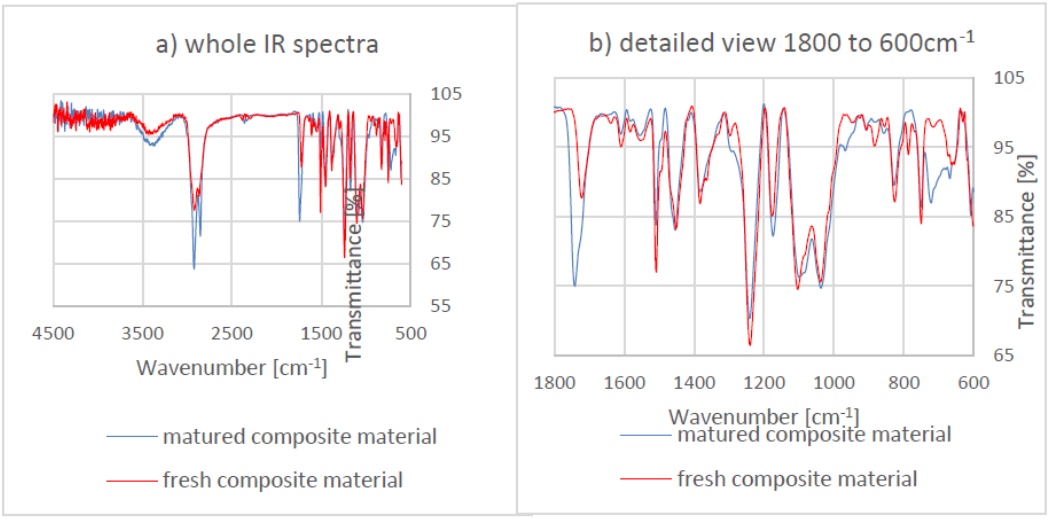


Fig. 7 – Comparison of IR spectra from aged and fresh composite material with a content 65% rosin and 50% epoxy resin: a) whole IR spectra; b) detailed view between 1800 and 600$cm^{-1}$.

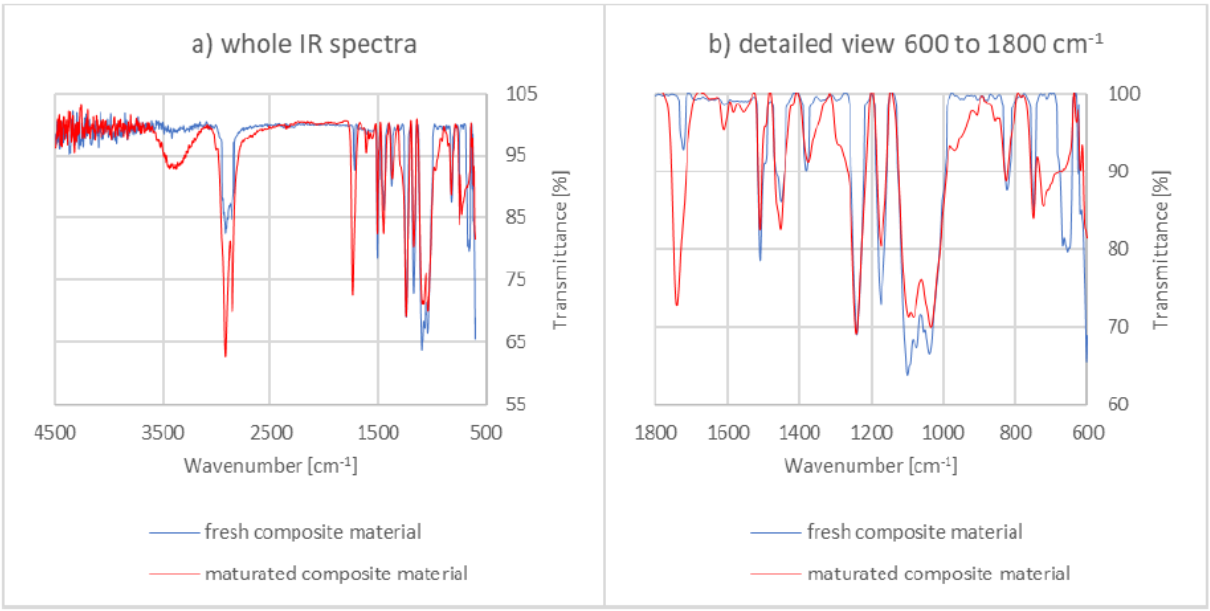


Fig. 8 – Comparison of IR spectra from aged and fresh composite material with a content 50% rosin and 50% epoxy resin: a) whole IR spectra; b) detailed view between 1800 and 600$cm^{-1}$.

In summary, the IR investigations show that the rosin is chemically involved in the polymerisation process. The interpretation of the IR spectra suggests that the acids of the rosin are initially present mainly as ammonium salts. In a subsequent ageing process, covalent bonding to the synthetic resin then occurs.

## EXPERIMENTAL

### Sample preparation

Rosin natural resin, which was bought commercially, is diluted with turpentine resulting a 10% solution and stored in a liquid state in closed containers. The hardening process of the diluted resin is very long. This disadvantage can be overcome by initiating the polymerization with the help of a synthetic resin, together with the related hardener. In this case, the

polymerization process was generated with Resoltech 1050 epoxy resin and the related Resoltech 1055 hardener (Scheme 1). This technique was already used for other biocompatible substances.[11] The technical data of Resoltech 1050/Resoltech 1055 (epoxy resin and hardener) can be found on the manufacturer's web page.[12]

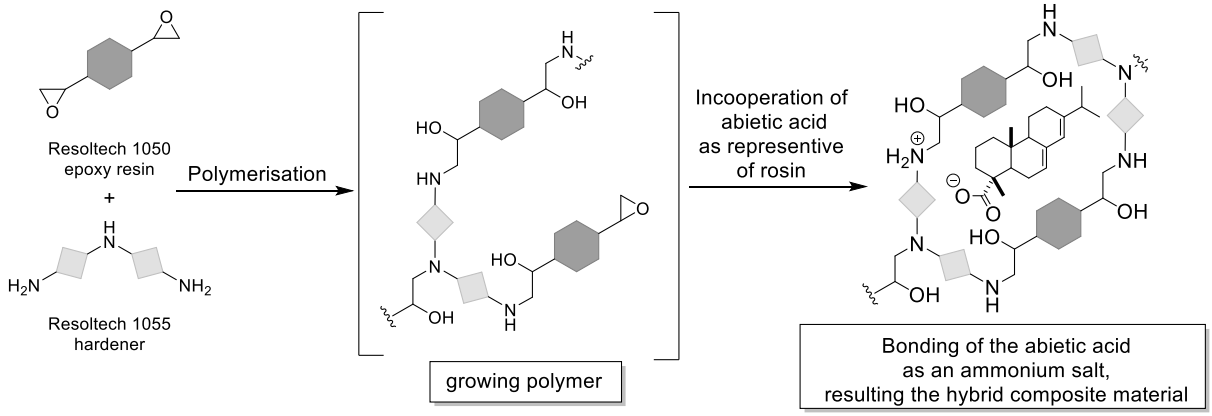


Scheme 1 – Polymerisation of Resoltech 1050 epoxy resin and the related Resoltech 1055 hardener in the presence of rosin.

Five types of hybrid resin samples were prepared with volume proportions of 45%, 50%, 55%, 60%, and 65%, natural Rosin resin. Furthermore, from the composites materials with contains 50% and 65% of rosin were maturated samples prepared. These two types of hybrids were prepared twelve months earlier and were stored at room temperature at atmospheric conditions. As a result of the preparation steps, it should be mentioned that volume proportions higher than 65% natural rosin resin were also tried: however, it was found that the curing time of the hybrid resin increased significantly (> 24 h). For this reason and the fact that the samples no longer hardened properly, we did not prepare hybrid resin samples with for rosin volume ratios greater than 65% as these no longer can be used for composite material applications.

Plates were cast from the three hybrid resins from which 10 samples/plates were cut, with dimensions of 250 mm × 25 mm × 8 mm. The specimens were tested in tension, which was carried out in compliance with the provisions of ASTM D3039. For the same three hybrid resins, rods were cast from which 10 cubes with a width of 21 mm were cut. These were requested in compression, which was carried out in compliance with the provisions of ASTM D695.

## Apparatus used

For the tensile stress, the LLOYD Instruments Lrx PLU mechanical testing machine was used, with a maximum force of 2.5 kN, a maximum travel of the crossbar of 1400 mm, strain gauge on 50 mm. The compression test was carried out with Walter-Bai LF300 universal static and dynamic testing machine, with the capacity of 300 kN. The loading speed was 250 N/s.

The solid-state NMR experiments were carried out using a Bruker Avance III console in combination with a Bruker Ascend 300WB magnet (7.05 T). The samples were measured using a magic-angle spinning (MAS) probe for 4 mm rotors at 10.0 kHz spinning frequency. The Cross Polarization-Reverse Insensitive Nuclei Enhanced by Polarization Transfer (CP-RINEPT)[13] NMR spectra were recorded using 4092 to 8192 scans, employing a relaxation delay of 6 s. The radio frequency (rf) pulses for the $^{13}C$ channel employed lengths of 5.0 μs (90° flip angle) and 10.0 μs (180° flip angle), corresponding to a rf field strength of $\nu_{rf} = 50.0$ kHz. The $^{1}H$ channel used rf pulses with a length of 4.17 μs (90° flip angle) and 8.34 μs (180° flip angle) corresponding to $\nu_{rf} = 60.0$ kHz. The duration of the CP contact pulse was varied between 2.5 and 3.0 ms. During the CP-acquisition part the protons were decoupled at $\nu_{rf} = 60.0$ kHz (CW) and during RINEPT-acquisition at $\nu_{nut} = 25.0$ kHz ($SW_fTPPM$). A Lorentzian line broadening of 30 Hz was applied to all recorded spectra. The data was processed using TopSpin 4.3 and plotted using Origin 2024.

Liquid $^{1}H$ and $^{13}C$ NMR spectra were recorded at room temperature on a Bruker Avance 300 operating at 300 MHz for $^{1}H$ and 75 MHz for $^{13}C$. Chemical shifts (δ) are reported relative to the tetramethylsilane peak (δ = 0.00 ppm).

Infrared (IR) spectra were measured on a Bruker Vertex 70 spectrometer using a PIKE MIRacle ATR

device with a ZnSe ATR crystal under ambient conditions.

## CONCLUSION

The change in mechanical properties depends very much on the ratio of natural resin and epoxy resin. The best values for the mechanical properties are achieved for the resin with 45% rosin. For the resin with 55% rosin content, the breaking strength is 48% and the modulus of elasticity is 34% This trend is reinforced for the resin with 65% rosin content (breaking strength 15 % and modulus of elasticity only 2%). However, the decrease in mechanical properties observed with increasing rosin content follows proportionality between the tensile strength or modulus of elasticity and the volume fraction of epoxy resin. The characteristic curves indicating the dependence of stress and specific strain are very different for the three types of hybrid resins. Although all show non-linearities from the beginning of the stress, in the case of the 65% rosin resin a flow phenomenon occurs, the elongation already increases strongly at a stress increase of 1 MPa. Similar conclusions are drawn for compressive stresses, with the hybrid resin with 45% rosin exhibiting the best behavior. In comparison, the maximum strength of the resin with 55% rosin is 62% and that of the resin with 65% rosin is 40%. For all the resins tested, the maximum compressive stresses were higher than the breaking strength values.

The analysis of the manufactured samples using solid-state $^{13}C$ NMR spectroscopy and infrared spectroscopy provided insights into the chemical structure and the bonding of the rosin to the epoxy resin. In particular, the comparison of freshly produced samples with aged samples provided important insights into the chemical dynamics. From solid-state $^{13}C$ NMR spectroscopy, a new signal is observed at $\delta = 177.7$ ppm, which is reduced in favour of a new signal at $\delta = 172.3$ ppm during ageing. A similar phenomenon is observed in IR. After production, a new dominant band is observed at 1240 $cm^{-1}$. During the ageing process, a strong band is formed at a wavenumber of 1740 $cm^{-1}$.

Combined the results can be explained by the fact that during the primary curing process, the epoxy resin is formed in which the acids of the rosin are ionically bound. In the subsequent ageing process, the acids are increasingly covalently bound to the epoxy resin via ester bonds (band at 1740$cm^{-1}$, Scheme 2). This bonding of the rosin to the epoxy resin supports the weakening of the stability of the composite materials and also explains the observed mechanical weakening of the hydride resin with increasing rosin content.

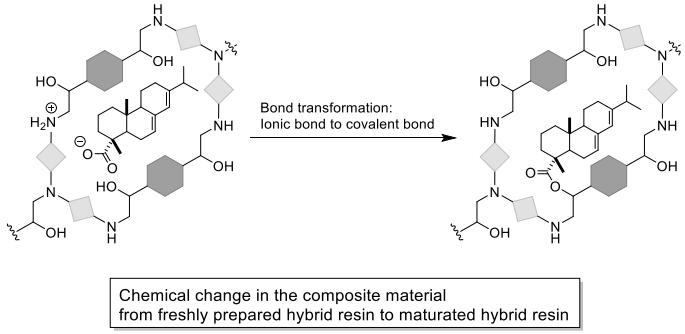


Scheme 2 – Bond transformation from an ionic bonding of the abietic acid to a covalent bonding.

*Acknowledgement.* We would like to thank Prof. Matthias Tamm, Institute of Inorganic and Analytical Chemistry, Technische Universität Braunschweig, for recording the NMR experiments of the monomers and performing the IR spectroscopic investigations of the polymers and discussing the results.

## REFERENCES

1. T. T. H. Nguyen, S. Li and J. Li, *Constr. Build Mater.*, **2013**, *40*, 33–39. https://doi.org/10.1016/j.conbuildmat.2012.11.010
2. H. R. Mansouri, A. Pizzi, J. M. Leban JM, Delmotte L, Lindgren O, Vaziri M., *J. Adhes. Sci. Technol.*, **2012**, *25*, 1987–1995. https://doi.org/10.1163/016942410X544794
3. Dong Y, Yan Y, Wang K, Li J, Zhang S, Xia C, Shi S, Cai L., *Eur. J. Wood Prod.*, **2016**, *74*, 177–184. https://doi.org/10.1007/s00107-015-0998-6
4. Fang X, Alvaro GH, Frank W, Pietro L., *J. Mater. Civ. Eng.*, **2016**, *28*, 04015199. https://doi.org/10.1061/ (ASCE)MT.1943-5533.0001454

5. D. H. Dai, C. Y. Sun, F. Y. Li, Y. J. Yang, X. G. Ren and Z. M. Wang, *Appl. Mech. Mater.*, **2012**, *204*, 3672–3676. https://doi.org/10.4028/www.scientific.net/AMM.204-208.3672
6. M. N. Belgacem and A. Gandini, "Monomers, polymers and composites from renewable resources." Elsevier Science, Amsterdam, 2008. https://doi.org/10.1016/B978-0-08-045316-3.X0001-4
7. V. Mahendra, *Appl. Mech. Mater.*, **2019** *890*, 77–91 https://doi.org/10.4028/www.scientific.net/AMM.890.77
8. G. Demircan, M. Kisa and M. Özen, *Emerg. Mater. Res.*, **2020**, *9*, 1076–1081 https://doi.org/10.1680/jemmr.20.00001
9. X. Liu, W. Xin and J. Zhang, *Bioresour. Technol.*, **2010**, *101*, 2520–2524 https://doi.org/10.1016/j.biortech.2009.11.028
10. D. Hu, X. Zhang, X. Liu, Z. Qin, L. Hu, C. Rudd and X. Yi, *J. Compos. Sci*. **2020**, *4*, 168 https://doi.org/10.3390/jcs4040168
11. M. H. Franz, I. Neda, C. V. Maftei, I. Ciuca, D. Bolcu and M. M. Stanescu, *Polym. Bull.*, **2021**, *78*, 2427–2438 https://doi.org/10.1007/s00289-020-03221-4
12. RESOLTECH 1050, hardeners 1053 to 1059. Structural Lamination Epoxy System. Available online: www.scabro.com/images/.../1/.../Resoltech%201050/DS-1050.pdf. (accessed on January 30, **2024**).
13. R. Zhang, K. H. Mroue and A. Ramamoorthy, *J. Magn. Reason.*, **2016**, *266*, 59–66 https://doi.org/10.1016/j.jmr.2016.03.006
14. A. Nowacka, N. A. Bongartz, O. H. S. Ollila, T. Nylander and D. Topgaard, *J. Magn. Reason.*, **2013**, *230*, 165–175 https://doi.org/10.1016/j.jmr.2013.02.016
15. K. Aebischer and M. Ernst, "INEPT and CP transfer efficiencies of dynamic systems in MAS solid-state NMR." *J. Magn. Reason.*, **2024**, *359*, 107617 https://doi.org/10.1016/j.jmr.2024.107617
16. S. Kugler, P. Ossowicz, K. Malarczyk-Matusiak and E. Wierznicka, *Molecules*, **2019**, *24*, 1651 https://doi.org/10.3390/molecules24091651
17. Q. Li, X. Huang, H. Li, S. Shang, Z. Song and J. Song, *RSC Adv.*, **2018**, *8*, 14684–14693 https://doi.org/10.1039/C7RA13672B